Available online at www.sciencedirect.com

ScienceDirect

Procedia CIRP 65 (2017) 78 – 83

www.elsevier.com/locate/procedia

3rd CIRP Conference on BioManufacturing

A study on degradation behavior of 3D printed gellan gum scaffolds

Ilhan Yu[a] ,Samantha Kaonis[b], Roland Chen[a,]*

[a]*School of Mechanical and Materials Engineering at the Washington State University, Pullman, WA, 99164*
[b]*School of Chemical Engineering and Bioengineering at the Washington State University, Pullman, WA, 99164*
* Corresponding author. Tel.: +1-509-335-0376; fax: +1-509-335-4662. *E-mail address:* roland.chen@wsu.edu

Abstract

Gellan gum (GG) is one of the natural hydrogels showing potential for tissue engineering. In this study, we investigate GG for wound dressing and cartilage applications through 3D printing which allows for the creation of complex structures and scaffolds with different porosities. Degradation of two different GG scaffold designs and one solid sample were performed using both simulated body fluid and phosphate buffered saline. It was found that the scaffolds with a higher surface area to mass ratio have a higher degradation rate, and that the compressive modulus and strength increase after degradation in simulated body fluid.

Peer-review under responsibility of the scientific committee of the 3rd CIRP Conference on BioManufacturing 2017

Keywords: 3D printing; cartilage; degradation; gellan gum; tissue engineering; wound dressing;

1. Introduction

Gellan gum (GG) is one type of hydrogel that has been used as a biomaterial for tissue engineering purposes. GG was discovered in 1978 and became available in the commercial market by C.P. Kelco in the U.S. and Japan [1]. GG is a natural polymer with repeating units consisting of α-L-rhamnose, β-D-glucose and β-D-glucoronate with molar ratios of 1:2:1 [2, 3]. The molecular form of GG is a threefold double-helical structure and under appropriate aqueous conditions, an aggregation of its double-helical structure causes a gel network leading to gelling [4]. It is known that different types of cations can influence gelation behavior in GG. Some examples are Na^{+}, K^{+}, Ca^{2+}, and Mg^{2+} [5, 6]. GG was originally used as a food thickener, but now is being used as a biomaterial in many applications such as ophthalmic formulations [11] and oral drug delivery [12].

Biomaterials for tissue engineering require biocompatibility, biodegradability, adequate porosity, sufficient water absorption, and suitable mechanical strength tailored to its application [7]. GG has great potential for many tissue engineering applications because of its easily tunable properties degradation rates and mechanical properties [6] as well as its heat and acid stability [8]. Researchers have been studying GG for tissue engineering applications such as wound dressings [8,12-14,19], artificial cartilage application [8-10, 16], and bone osteogenesis [17]. GG has the desirable properties for wound dressings including soft texture and tunable mechanical properties [18]. GG can crosslink with other chemicals and encapsulate drugs for wound dressing [19]. GG has also been considered as a potential solution for cartilage regeneration, but this application remains a challenge topic because of cartilage tissue's poor self-repair capability [17].

Manufacturing of GG for wound dressing or cartilage applications is difficult because complex structures are needed for these purposes, such as for patient-specific geometries or organ mimicking designs. This difficulty is because of GG's soft texture and temperature sensitive properties. 3D printing has become a solution to this manufacturing problem, and the printability of GG has been established by previous research [14]. 3D printing not only makes manufacturing of GG more feasible but it also allows for the control of porosity. Being able to control the porosity is beneficial for wound dressing applications because the drug delivery rate as well as the degradation rate can be changed by different porosities or surface areas and customized for individual patients [20]. Previous research demonstrates how degradation rate is

Peer-review under responsibility of the scientific committee of the 3rd CIRP Conference on BioManufacturing 2017
doi:10.1016/j.procir.2017.04.020

affected by changing the concentration of GG or its crosslinking method, however, the effects of changing porosity on degradation rate have not yet been studied. Chemical reactions between the GG and chemicals within the body fluid during degradation may change the mechanical properties of material because GG is sensitive to the ions that are naturally in the human body [2]. Knowing how the hydrogel will respond to the body is important because it could exhibit different properties over time. Whether the structure becomes stronger or weaker *in vivo* compared to the original design, can be critical for both wound dressing and cartilage replacement purposes. [6, 10]. For example, if artificial cartilage degrades faster than expected, it will not provide the needed mechanical properties.

The purpose of this study is to determine how 3D printed GG can be applied to wound dressing or cartilage replacement applications. In this study, we will perform degradation tests with phosphate buffered saline (PBS) and simulated body fluid (SBF) which are intended for wound dressing and cartilage replacement applications, respectively. Degradation rates of scaffolds with different porosities will be measured, and compression tests will also be performed in order to determine how the mechanical properties change throughout degradation.

2. Materials and Methods

2.1. Material

In this research, the gellan gum powder, Gelrite (G1910, Sigma-Aldrich, St. Louis, MO, USA), was used to fabricate the hydrogel. The powder was used as it was received. Ultra-pure water (18.2MΩ) purified by Barnestead Water Purification System (Dubuque, Iowa, USA) was used for all solutions in this study. Two mediums were used for the degradation tests, PBS and SBF.

To prepare PBS, a PBS tablet (P4417, Sigma-Aldrich) was dissolved in ultra-pure water. The solution's pH value (pH 7.4 at 25 °C) was checked for concentration. SBF was prepared following the protocol by Tas [21]. The chemicals for producing SBF, NaCl (99.5%), $NaHCO_3$ (99.5%), KCl (99.0%), Na_2SO_4 (99.0%), $Na_2HPO_4 \cdot 2H_2O$ (99.5%), $MgCl_2 \cdot 6H_2O$(99.0%),$CaCl_2 \cdot H_2O$(99.0%), $(CH_2OH)_3CNH_2$ (99.5%), and HCl (37 vol%) were all acquired from Sigma-Aldrich.

2.2. Preparation of hydrogel

The GG powder was mixed with ultra-pure water (2% w/v), and heated in a water bath (Digital constant temperature tank, HH-2) at 90°C for 30 min while stirring occasionally. For the solid samples, the heated GG solution was poured directly into a mold and cooled to room temperature. The solid samples had a 5-mm thickness and a diameter of 12 mm on the top and 10 mm on the bottom. The bottom of the sample was made smaller for easier demolding. For 3D printing, the hydrogel was poured into a syringe (3 cc) maintained at 53°C in the water bath before the printing process.

2.3. 3D Printing process

The GG scaffold was printed with the Inkredible Bioprinter (Cellink, Gothenburg, Sweden). A custom heating system, as shown in Fig.1, was added to the printhead to maintain the hydrogel solution at the desired temperature for printing. The heating system includes a 5W heating film, a conductive copper sleeve, a thermistor, a temperature controller (Arduino UNO R3 Mega 2560, Glendora, CA, USA), and a DC power supply. The thermistor was attached on the surface of the conductive copper sleeve. The nozzle tip used was a 21-gauge needle. The power supply was also directly connected to the nozzle tip for heating to prevent the hydrogel solution from solidifying inside the nozzle.

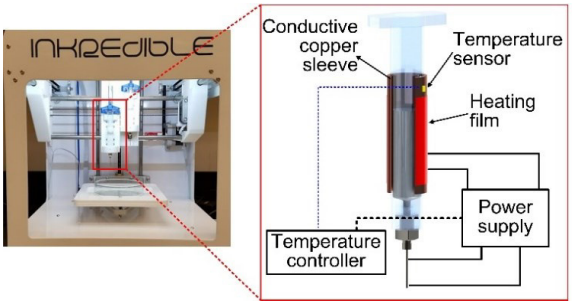

Fig. 1. 3D printing setup with modified printhead

The Inkredible Bioprinter uses a pneumatic extrusion system and a pressure of 7 to 11 kPa was used to print the hydrogel scaffolds. Two scaffold designs were fabricated. The two designs had either 3 mm or 4 mm distances between two adjacent tool paths. The size of the scaffolds was 24 mm by 24 mm with a total of 12 layers (total thickness of 2 mm). The tool path of the 3 mm design is illustrated in Fig.2. The feed rate used was 800 mm/s (solid lines in Fig. 2) for the longer toolpath and a faster feed rate 1800 mm/s (dash lines in Fig.2) at each turning point when the toolpath overlapped with next layer, to prevent excessive material deposition at the shorter edges and corners. The scaffolds were directly printed onto glass petri dishes that were then used for the degradation test.

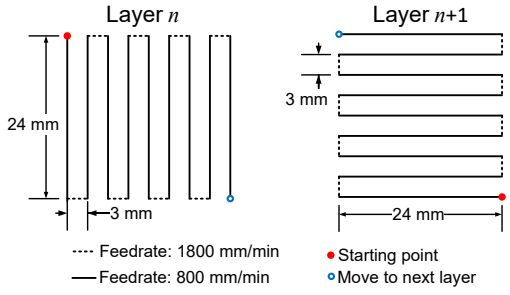

Fig. 2. Printing tool path of the scaffold.

2.4. Calculation of Surface Area

The surface area of the scaffold was estimated based on a reconstructed 3D model using SolidWorks 2015 (Dassault Systems, Vélizy-Villacoublay, France), because of the practical difficulties in measuring the actual surface area. Figs. 3(a) and (b) illustrate the parameters needed in order to reconstruct the model of a scaffold, including line width (w), corner radius (r_1), and corner radius of pores (r_2). With the printing process described above, the average line width of printed hydrogel on the petri dish is determined to be 1.73 mm, as shown in Fig. 3(a). Fig. 3(c) shows the top view of the reconstructed 3D model of the 3 mm scaffold.

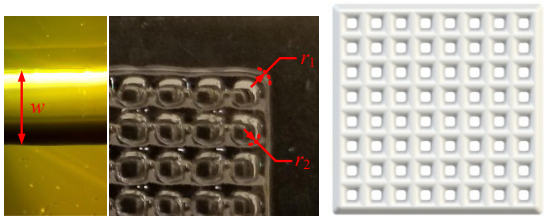

(a) (b) (c)

Fig. 3. Reconstruction of the 3D model the scaffold: (a) line width of the scaffold, (b) corner radii, and (c) the reconstructed 3D model of the scaffold

2.5. Degradation Test

For the degradation test, samples with three different porosities were tested, including solid samples and scaffolds with 3 and 4 mm designs. Two degradation mediums, PBS and SBF, were used. For wound dressing applications, degradation is often performed in PBS, while SBF is commonly used for degradation test of ceramics and engineering cartilage materials.

Each petri dish was weighed before and after the scaffold was printed to determine the initial weight of the scaffold. 50 ml of PBS or SBF was poured into each petri dish to immerse the sample. The period for the degradation test is 21 days. First, five data points were measured every 4 hours right after the scaffold is printed (4, 8, 12, 16, and 20 hours) to observe rapid initial degradation or swelling effects. After this, 12 data points were collected at 1, 2, 3, 4, 5, 6, 7, 10, 13, 16, 19, and 21 days. One hydrogel sample was tested for each data point. During the test, the samples in the petri dishes were maintained at 37°C in an incubator (RS-IF-233, Revolutionary Science, Shafer, MN, USA). The degradation rate is calculated based on Equation 1

$$\text{Degradation rate} = \frac{(m_o - m_d)}{m_o} \cdot 100\ \% \qquad (1)$$

where
m_o= original weight
m_d= weight after degradation

2.6. Compression Test

It is important to compare and identify any changes in mechanical properties before and after the degradation. Since there are no ASTM or ASM standards for compression test of hydrogels or soft materials, the dimensions of the sample were chosen by the authors. The samples had a diameter of 18 mm and a height of 6 mm. Three different samples were prepared and tested, including samples after 7-day degradation in both PBS and SBF, and a non-degraded sample. Mark-10 ESM303 (Mark-10 Corporation, NY, USA) was used to perform this compression test with a strain rate of 0.02 s^{-1}.

3. Results

3.1. Scaffolds and samples

Fig. 4 shows the fabricated scaffolds. Table 1 lists the physical characteristics of the samples. The average weight of sample was 0.432 g for the 3 mm scaffold, 0.519 g for the 4 mm scaffold, and 0.450 g for the solid sample.

The estimated surface areas of all sample designs are listed in Table 1. The surface area of scaffolds was around five times bigger than that of the solid sample. The surface area of the 3 mm scaffold is 9.5% larger than that of the 4 mm scaffold.

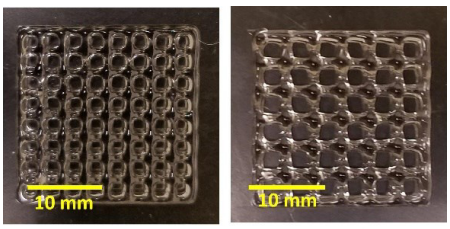

3 mm scaffold 4 mm scaffold

(a) (b)

Fig. 4. Fabricated scaffolds: (a) 3 mm scaffold, (b) 4 mm scaffold,

Table 1. Average weight, surface area, and ratio

	Average weight (g)	Surface area (mm^2)	Surface area per mass (g/mm^2)
Solid	0.450	367	817
3 mm sample	0.439	1753	4040
4 mm sample	0.490	1600	3295

3.2. Degradation test

Fig. 5 shows the samples after degradation in PBS and SBF. After the degradation test, the color of samples immersed in SBF turned white. However, the color of samples degraded in PBS didn't change. The degradation results of GG hydrogel in SBF and PBS are presented in Fig. 6. In the

first 24 hours, the solid sample show a very linear curve, but the solid sample lost more than 10% of its original weight after 21 days in both solutions. Solid sample immerged in SBF degrade faster than sample immerged in PBS. The solid sample in SBF reaches around 90% of original weight in 24 hours and slowly decreased to 86% after 21 days. The sample in PBS shows slower and lower degradation than sample in SBF.

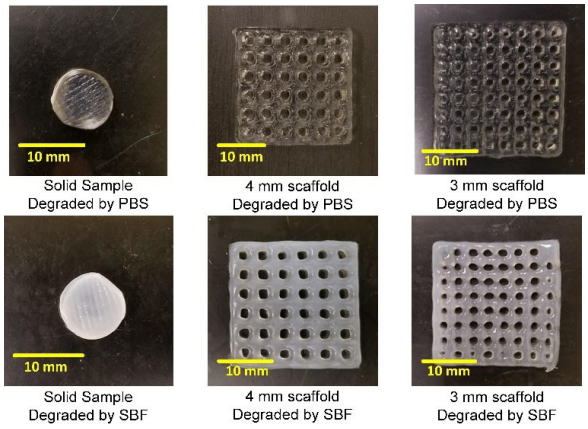

Fig. 5. Samples degraded by PBS (top) and SBF (bottom).

The 3 mm and 4 mm scaffolds lost about 25-30% of its original weight in the first four hours in both SBF and PBS. There was no significant difference in degradation rate between 3 mm and 4 mm samples. However, samples in SBF are observed to show slightly faster degradation rate than samples in PBS. The samples showed the fastest degradation rate is 3 mm immerged in SBF.

Fig. 7 shows the relationship between surface area/mass and each sample's average degradation. In general, there is a linear trend as surface area/mass ratio increases, degradation also increases. Also, samples immersed in SBF show higher degradation than those in PBS. Solid samples have the smallest surface area/mass ratio and also fewest degradation, 8.10 % in PBS and 10.11 % in SBF. The 3 mm scaffolds have higher surface area/mass ratio and larger degradation than the 4 mm scaffolds, when compared to the results in the same degradation medium.

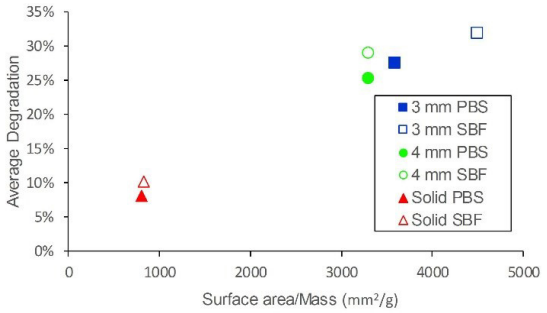

Fig. 7. Ratio of surface area to mass versus average degradation.

3.3. Compression Test

Fig. 8 shows the stress-strain curves for the compression test of samples degraded in SBF and PBS, and the non-degraded samples. Samples immersed in SBF had an ultimate compressive strength more than 10 times higher (223 kPa) than that of the non-degraded samples (20 kPa). Samples immersed in PBS also showed an increased compressive strength (34 kPa). However, samples degraded in SBF failed at 0.57 mm/mm strain while PBS and non-degraded samples failed at 0.66 mm/mm and 0.69 mm/mm, respectively.

Fig. 9 shows the compressive moduli of samples degraded in SBF and PBS and non-degraded samples. The compressive modulus was calculated at 0.45 mm/mm strain. The samples immersed in SBF shows 14.5 times higher compressive modulus than the non-degraded samples. The compressive modulus of samples immersed PBS increased 137% compared to the non-degraded samples.

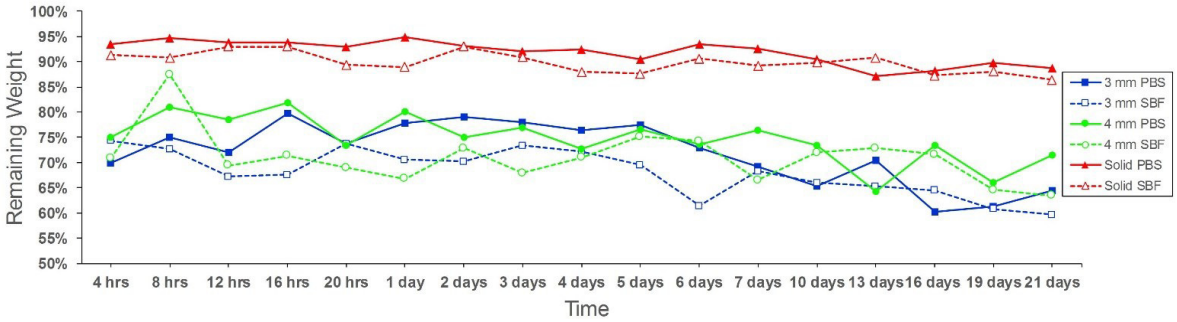

Fig. 6. Degradation results over the 21-day period.

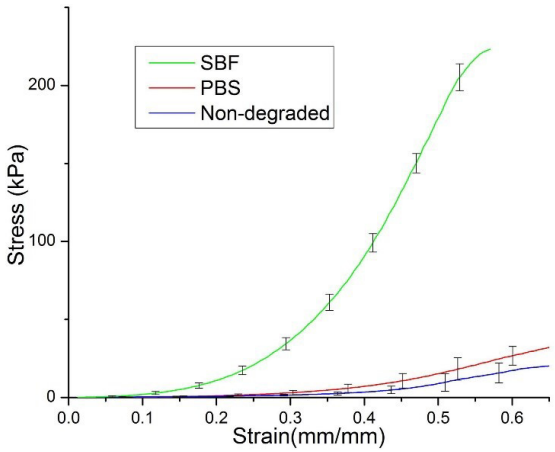

Fig.8. Stress-strain curves of gellan gum samples.

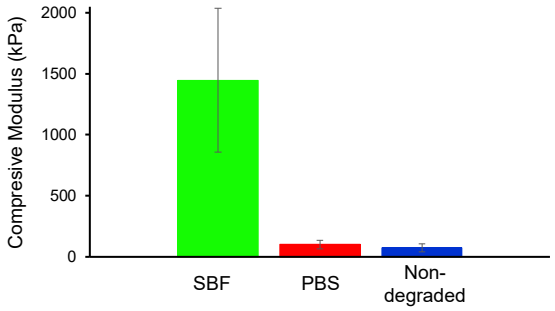

Fig. 9. Compressive moduli of samples with and without degradation.

4. Discussion

The main goal of this study is to determine the effect of surface area per mass, i.e. porosity, on the scaffold's degradation rate. This effect can clearly be seen in Fig. 7 where higher surface area per unit mass led to a faster degradation rate in both solutions. The surface area of a 3 mm sample is around 5 times bigger than that of a solid sample, while the scaffold samples had about three times of the percentage of degradation than that of the solid sample. There is only a 10 % difference in surface area/mass between the 3 mm and 4 mm scaffolds, and the difference in degradation is not significant. However, when comparing the results in the same degradation solution, samples in SBF show a larger degradation.

In this study, the surface area of the scaffold was estimated by reconstructing a 3D model of the scaffold with three parameters and the defined tool path. It is technically very challenging to experimentally measure the surface area. To evaluate the usefulness of this method of estimation, a sensitive analysis was performed. It was determined that the surface area of the scaffold was not very sensitive to the corner radii. The spacing between each tool path is the most important factor affecting the surface area. Although the line width and corner radii are not constant over the scaffold, the calculation based the 3D model still provides a reasonable estimation of the surface area.

From the results, GG, when degraded in PBS, has a suitable degradation rate for wound dressing purposes. With a 3-week test period, the lowest point was 60.3 % of original weight. Also, the compressive modulus of GG shows that GG in PBS still retains its soft texture even though it increased by 137 %.

Fig.8 shows how compressive strength changes during degradation. The sample immersed in SBF failed at 223 kPa which is more than eleven times higher than the failing point of the non-degraded sample. On the other hand, strain at which failure occurred decreased from 0.69 mm/mm to 0.57 mm/mm. This shows that the sample immersed in SBF becomes more brittle, yet still retaining a higher compressive strength and modulus than the non-degraded samples. The sample immersed in PBS does not show as much of a difference in failure strength as samples in SBF, but the compressive modulus was 1.7 times higher than the non-degraded samples, with a failure strain rate decrease to 0.66 mm/mm.

GG has the tendency to become stiffer and harder during the degradation test using SBF. Moreover, it could lose more than 40 % of its original weight during 3 weeks. This degradation rate is too fast when considering the slow recovery speed of cartilage. On the other hand, by crosslinking with cations in SBF, compressive modulus and strength of GG increased. One of main focuses of GG for cartilage replacement applications is to try to increase the mechanical properties. Having more surface area with higher porosity would result in an increased speed of crosslinking with the ions in the body, which can lead to a stiffer and stronger scaffold. However, the degradation rate also increases when the surface area increases becoming a tradeoff to think about when considering GG for cartilage engineering purposes.

There are several limitations in this study. First, there are variations in the measurement of the remaining weight during the degradation test. Before the degraded samples can be weighed, the surface of the samples has to be dried. The scaffold contains lots of water and the structure of scaffold makes it difficult to clean up the solution on the surface. Any residual solution or over drying can introduce measurement errors. One way to improve this is to measure the dry weight of the scaffold, by desiccating the samples. This requires the knowledge of the initial dry weight of each sample which can be challenging.

Second, previous studies by other groups did not observe GG degradation in PBS and that any degradation may be contributed to water loss [6]. In order to differentiate the effect of water loss from actual degradation, the measurement of the dry weight of the samples will be required. Third, the surface area of the scaffold was estimated using a reconstructed 3D model and there would exist some minor errors in the estimation. For a tighter comparison, a more accurate method of estimating the surface area will be needed.

5. Conclusions

This study shows that the degradation rate of gellan gum can be altered by changing the ratio of surface area per mass. Using 3D printing, it is possible to create scaffolds with different surface area per mass ratios. Therefore, GG is suitable for wound dressing applications because its degradation behavior can be tailored to allow for the control of temporal drug delivery. For cartilage applications, the faster degradation rate in SBF and changes in mechanical properties due to degradation makes GG, with any modification, a less ideal material for this purpose. In the future, scaffolds can be fabricated with different ratios of surface area to mass between that of the solid sample and the 3 mm and 4 mm scaffolds studied in this work. This would give us a better understanding about the correlation between surface area per mass and degradation rate. It will be possible to predict degradation rate based on the scaffold's porosity. Also, more studies can be conducted to determine how mechanical properties of the scaffold change during degradation test.

Acknowledgements

The authors would like to thank for partial support from NSF CMMI Grants #1642565 for this study.

References

[1] K. S. Kang, G. T. Veeder, P. J. Mirrasoul, T. Kaneko, and I. W. Cottrell, "Agar-like polysaccharide produced by a Pseudomonas species: production and basic properties," *Appl. Environ. Microbiol.*, vol. 43, no. 5, pp. 1086–1091, 1982.

[2] E. R. Morris, K. Nishinari, and M. Rinaudo, "Gelation of gellan – A review," *Food Hydrocoll.*, vol. 28, no. 2, pp. 373–411, Aug. 2012.

[3] P.-E. Jansson, B. Lindberg, and P. A. Sandford, "Structural studies of gellan gum, an extracellular polysaccharide elaborated by Pseudomonas elodea," *Carbohydr. Res.*, vol. 124, no. 1, pp. 135–139, 1983.

[4] R. Chandrasekaran, L. C. Puigjaner, K. L. Joyce, and S. Arnott, "Cation interactions in gellan: an X-ray study of the potassium salt," *Carbohydr. Res.*, vol. 181, pp. 23–40, 1988.

[5] E. Miyoshi, T. Takaya, and K. Nishinari, "Rheological and thermal studies of gel-sol transition in gellan gum aqueous solutions," *Carbohydr. Polym.*, vol. 30, no. 2–3, pp. 109–119, 1996.

[6] D. F. Coutinho *et al.*, "Modified gellan gum hydrogels with tunable physical and mechanical properties," *Biomaterials*, vol. 31, no. 29, pp. 7494–7502, Oct. 2010.

[7] T. Billiet, M. Vandenhaute, J. Schelfhout, S. Van Vlierberghe, and P. Dubruel, "A review of trends and limitations in hydrogel-rapid prototyping for tissue engineering," *Biomaterials*, vol. 33, no. 26, pp. 6020–6041, Sep. 2012.

[8] M. Rinaudo, "Role of substituents on the properties of some polysaccharides," *Biomacromolecules*, vol. 5, no. 4, pp. 1155–1165, Jul. 2004.

[9] C. Cencetti *et al.*, "Preparation and characterization of antimicrobial wound dressings based on silver, gellan, PVA and borax," *Carbohydr. Polym.*, vol. 90, no. 3, pp. 1362–1370, Oct. 2012.

[10] M.-W. Lee, H.-J. Chen, and S.-W. Tsao, "Preparation, characterization and biological properties of gellan gum films with 1-ethyl-3-(3-dimethylaminopropyl)carbodiimide cross-linker," *Carbohydr. Polym.*, vol. 82, no. 3, pp. 920–926, Oct. 2010.

[11] M.-W. Lee, H.-F. Tsai, S.-M. Wen, and C.-H. Huang, "Photocrosslinkable gellan gum film as an anti-adhesion barrier," *Carbohydr. Polym.*, vol. 90, no. 2, pp. 1132–1138, Oct. 2012.

[12] F. Wang, Y. Wen, and T. Bai, "The composite hydrogels of polyvinyl alcohol–gellan gum-Ca2+ with improved network structure and mechanical property," *Mater. Sci. Eng. C*, vol. 69, pp. 268–275, Dec. 2016.

[13] S. S. Mohd, M. A. A. Abdullah, and K. A. M. Amin, "Gellan gum/clay hydrogels for tissue engineering application: mechanical, thermal behavior, cell viability, and antibacterial properties," *J. Bioact. Compat. Polym. Biomed. Appl.*, p. 883911516643106, 2016.

[14] V. H. M. Mouser, F. P. W. Melchels, J. Visser, W. J. A. Dhert, D. Gawlitta, and J. Malda, "Yield stress determines bioprintability of hydrogels based on gelatin-methacryloyl and gellan gum for cartilage bioprinting," *Biofabrication*, vol. 8, no. 3, p. 35003, Jul. 2016.

[15] D. A. De Silva, L. A. Poole-Warren, P. J. Martens, and M. in het Panhuis, "Mechanical characteristics of swollen gellan gum hydrogels," *J. Appl. Polym. Sci.*, vol. 130, no. 5, pp. 3374–3383, Dec. 2013.

[16] J. T. Oliveira *et al.*, "Gellan gum: A new biomaterial for cartilage tissue engineering applications," *J. Biomed. Mater. Res. A*, vol. 9999A, p. NA-NA, 2009.

[17] M. B. Oliveira, C. A. Custódio, L. Gasperini, R. L. Reis, and J. F. Mano, "Autonomous osteogenic differentiation of hASCs encapsulated in methacrylated gellan-gum hydrogels," *Acta Biomater.*, vol. 41, pp. 119–132, Sep. 2016.

[18] R. Shukla, S. K. Kashaw, A. P. Jain, and S. Lodhi, "Fabrication of apigenin loaded gellan gum–chitosan hydrogels (ggch-hgs) for effective diabetic wound healing," *Int. J. Biol. Macromol.*, vol. 91, pp. 1110–1119, Oct. 2016.

[19] X. Cui and T. Boland, "Human microvasculature fabrication using thermal inkjet printing technology," *Biomaterials*, vol. 30, no. 31, pp. 6221–6227, Oct. 2009.

[20] M. Vallet-Regí, F. Balas, and D. Arcos, "Mesoporous Materials for Drug Delivery," *Angew. Chem. Int. Ed.*, vol. 46, no. 40, pp. 7548–7558, Oct. 2007.

[21] A. Cüneyt Tas, "Synthesis of biomimetic Ca-hydroxyapatite powders at 37°C in synthetic body fluids," *Biomaterials*, vol. 21, no. 14, pp. 1429–1438, Jul. 2000.